Pathway-dependent gold nanoparticle formation by biocatalytic self-assembly

Jugal Kishore Sahoo[a, b], Sangita Roy[a], Nadeem Javid[a, c], Krystyna Duncan[a], Lynsey Aitken[a], and Rein V. Ulijn[d, e, f]*

[a] WestCHEM, Department of Pure and Applied Chemistry, Technology and Innovation Center, University of Strathclyde, Glasgow, G1 1RD, UK
[b] Current Address: Department of Chemical and Biomolecular Engineering, McCourtney Hall, University of Notre Dame, IN, 46556, USA.
[c] School of Chemistry and Biosciences, University of Bradford, UK.
[d] Advanced Science Research Center at the Graduate Center of the City University of New York, 85 Saint Nicholas Terrace, New York, NY 10031, USA.
[e] Ph.D. programs in Biochemistry, Chemistry and Physics. The Graduate Center of the City University of New York, NY 10016, USA.

[f] Department of Chemistry, Hunter College, City University of New York, 695 Park Avenue, New York, NY 10065, USA

We report on the use of non-equillibrium biocatalytic self-assembly and gelation to guide the reductive synthesis of gold nanoparticles. We show that biocatalytic rates simultaneously dictate supramolecular order and presentation of reductive phenols which in turn results in size control of nanoparticles that are formed.

INTRODUCTION

Supramolecular self-assembly provides tremendous opportunities for design of functional materials with tunable properties.[1-4] In addition to chemical design of building blocks, it is increasingly appreciated that the self-assembly pathway determines structure (and therefore function). This is especially the case for gel phase materials which have restricted molecular dynamics and are easily locked in various kinetically trapped states.[5-10] (Bio-) catalytic self-assembly of supramolecular gels[11-13] provides a convenient approach to enable kinetic control of supramolecular structures by simply varying the catalyst concentration[14], which controls the rate of production of self-assembling building blocks from non-assembling precursors. The supramolecular structures formed may provide opportunities to control chemical reactions in dynamic nanostructured environments. Indeed, it has been demonstrated that transient formation of nanoparticle aggregates opens up new opportunities to control chemical reactions in dynamically changing confined space.[15]

Noble metal nanoparticles are of interest to a wide range of applications in sensing, imaging, therapeutics and diagnostics due to their size-tunable optical properties.[16, 17] There is a growing interest in soft templating approaches for the synthesis of these nanomaterials[18-21] Molecular self-assembly approaches, including a number of organogelators[22, 23] and hydrogelators[24, 25] have been used for shape-controlled synthesis of the gold nanoparticles. Peptides and peptide derivatives provide promising templating materials for directing the nanoparticle formation due to their self-assembly propensity and chemical versatility[19] potentially enabling templates with precisely controlled chemical functionality and structure. In addition to spatial features, which may be influenced by templating, kinetic aspects are key to the controlled formation of particles of defined size. In this context, biocatalytic growth of gold NPs in presence of glucose/glucose oxidase was reported, [26] where biocatalytic formation of H_2O_2 controls the growth of gold nanoparticles.

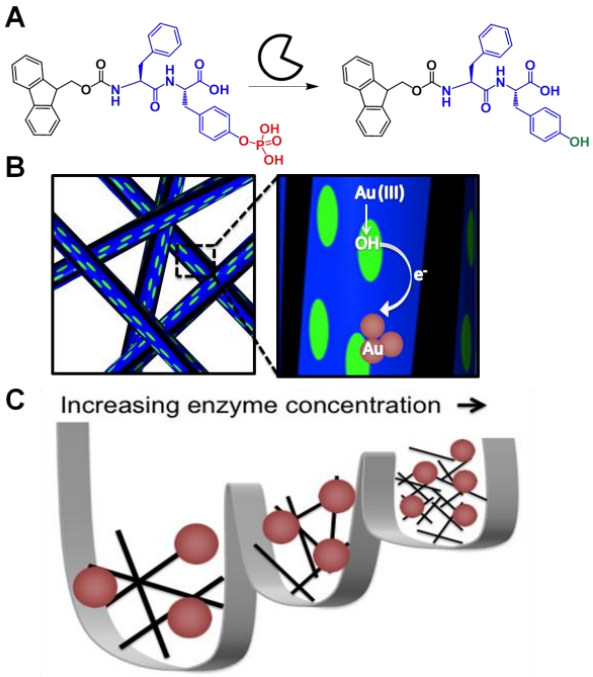

Figure 1. (A) Biocatalytic hydrolysis of Fmoc-FY*p*-OH to form self-assembling Fmoc-FY-OH. (B) Reduction of the gold chloride Au (III) to gold nanoparticle Au(0) in the hydrogel template where a coupled electron transfer mechanism occurs at –OH group of tyrosine. (C) Schematic of free energy landscape showing kinetic controlled fiber formation and nanoparticle reduction at different phosphatase concentrations.

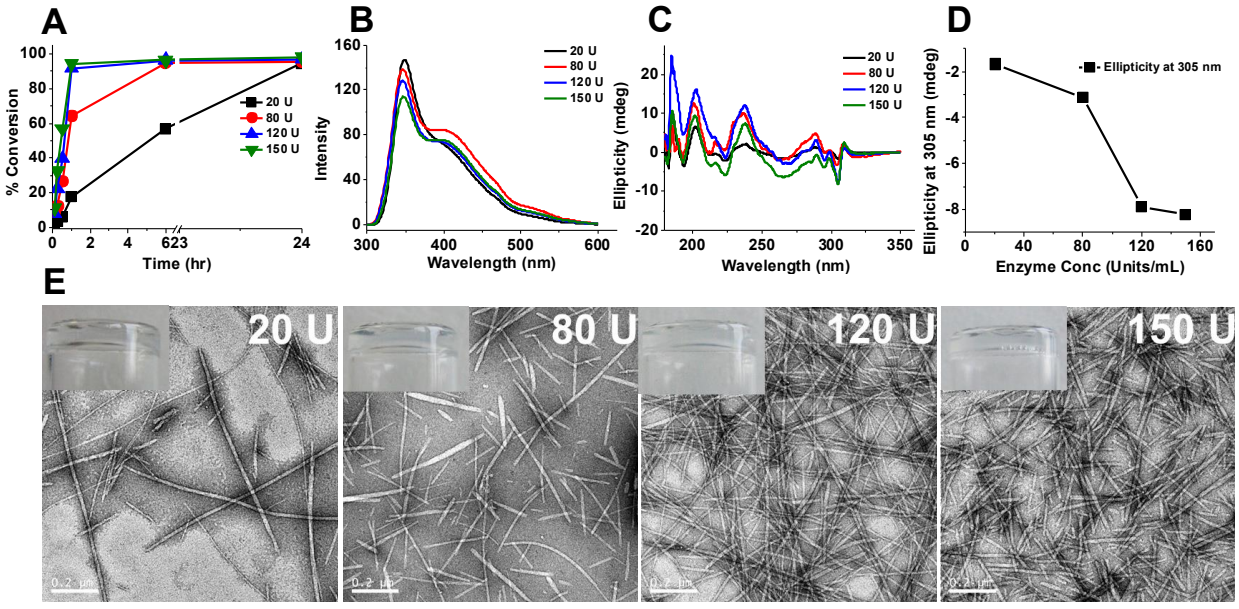

Figure 2: Biocatalytic self-assembly enables pathway controlled assembly and gelation. A) HPLC results for the enzymatic dephosphorylation, at different enzyme concentrations. At all enzyme concentrations, > 90 % peptide conversion was eventually observed so the final concentration of Fmoc-FY is similar in each system. B) Fluorescence spectroscopy after 24h of addition of enzyme at different concentrations. C) Corresponding Circular Dichroism (CD) spectra. (D) With increase in enzyme concentration there is enhancement of peak due to Fmoc- moiety (305 nm). (E) Transmission electron microscopy data of the nanofibers at different enzyme concentrations. One unit (U) will hydrolyze 1.0 µM of P-Nitrophenyl Phosphate to P-Nitrophenol and Phosphate at pH 9.8 at 37 °C; corresponds to 1 µl.

Existing methods till now, aimed at obtaining size control of nanoparticles formation typically focused on changes in chemical structures of templating agents. Here, we introduced a kinetic element of organic templating of inorganic nanoparticles formation where the chemical structures are identical, but their conversion to nanostructured fiber varies which give rise to kinetic control. In brief, we demonstrate the use of biocatalytic assembly to control simultaneously the rate of production of self-assembling structures and presentation of reductive phenol groups by dephosphorylation- this results in a tunable reaction environment, giving rise to kinetic controlled templating to control the size and optical properties of metal nanoparticles grown in gels (Figure 1).

The supramolecular hydrogel system used for the study was based on a previously reported aromatic dipeptide amphiphile,[27] where the dipeptide sequence was phenylalanine-tyrosine (FY), which was connected at the N-terminus to the hydrophobic aromatic fluorenylmethoxy carbonyl (Fmoc) group. We previously demonstrated the supramolecular transition from a micellar solution to a fibrous hydrogel network.[28] Upon dephosphorylation by alkaline phosphatase (ALP) Fmoc-FY self-assembles through a combination of π-π stacking between the Fmoc groups as well as hydrogen bonding interactions between the peptide backbones[27] to form a fibrous network, resulting in gelation.

First, kinetic controlled supramolecular gelation was studied, by simply varying the biocatalyst concentration in biocatalytic self-assembly of Fmoc-FY. The concentration of phosphatase was varied to influence the rate of hydrolysis of the phosphate ester to obtain kinetic pathway control, as previously demonstrated using a related (bio-)catalytic self-assembly approach.[11] A range of enzyme concentrations was used from 20-150 U (One unit (U) will hydrolyze 1.0 µM of P-Nitrophenyl Phosphate to P-Nitrophenol and Phosphate at pH 9.8 at 37 deg C; corresponds to 1 µl). The yield of the final hydrolyzed product was analyzed by high pressure liquid chromatography (HPLC). In each case, a near-complete conversion was observed (~90%) within 24 h, irrespective of enzyme concentration, indicating that final concentrations of gelator were identical (**Figure 2A**). As expected, the biocatalytic conversion rate was found to be significantly influenced by the phosphatase concentration. Stable, self-supporting gels were observed (**Figure 2E** (inset)) in each case. To assess the effects of assembly kinetics on molecular self-assembly at different phosphatase concentrations, we performed fluorescence spectroscopy (**Figure 2B**) after 24h of phosphatase addition to the reaction precursor (Fmoc-FY*p*-OH). With increase in phosphatase concentration, the fluorescence intensity due to Fmoc- moiety decreases (as indicated by quenching at 348 nm band), indicating the formation of Fmoc-aggregates.[28] In addition to fluorescence spectroscopy, Circular Dichroism (CD) spectroscopy was performed, in order to gain insights into the supramolecular chiral environments of the aromatic chromophore (Fmoc-) within the self-assembled structures of Fmoc-FY-OH at different concentrations of phosphatase. CD spectra (**Figure 2C**) can provide information on the relative orientation of fluorenyl- moiety in the self-assembled supramolecular structures through its characteristics CD signals at 305 nm.[11] From the CD results it can be concluded that with increase in phosphatase concentration, supramolecular chirality of the self-assembled structures is systematically enhanced (**Figure 2D**).[10]

Nanoscale morphology was characterized using transmission electron microscopy (TEM), revealing nanofiber-like morphology with varying lengths up to micrometer scale and 20-30 nm in diameter (**Figure 2E, S6**). At lower phosphatase concentration (20 and 80 U/mL) relatively longer, thicker and less dense nanofibers were observed. At higher phosphatase concentrations (120 and 150 U/mL) thinner, shorter nanofibers were observed with higher fibrous density (**Figure S6**). Similar behavior of the nanostructures (longer fibers at lower enzyme concentrations) was previously observed using variable esterase concentrations to trigger supramolecular assembly of Fmoc-dipeptides.[11] Thus, despite similar hydrogelator composition after 24h (> 90 %), the morphology and physical and chemical properties of the hydrogels can be tuned by controlling the rate of self-assembly (*i.e.* rate of dephosphorylation) by changing the concentration of biocatalyst.[12]

Tyrosine was used previously as an effective reducing agent[29, 30] for Au (III) to Au (0). We explored the possibility of using enzymatically produced Fmoc-FY-OH as *in situ* formed reducing agent for Au (III), followed by the stabilization of the particles by the formed nanostructures (**Figure 1**). We envisage that the dynamics of the biocatalytic self-assembly process can be utilized in the controlled synthesis of gold (Au) nanoparticles. Reduction was carried out under physiological conditions by adding yellow colored Au (III) chloride solution (20 µl; 50 mM) at the start of the assembly process. The color changed from yellow to pink/purple within 24-48h, depending up on the enzyme concentration, suggesting a controlled generation of the nanoparticles (**Figure 3A**) which could be related to the self-assembly kinetics at different phosphatase concentrations. At lower phosphatase concentration (20 U), a change in colour was observed (from yellow to purple) in absence of gelation. At higher phosphatase concentrations, we observed coloured,self-supporting hydrogels (**Figure 3A**). The effect of the dynamics of the self-assembly was also reflected in the surface plasmon resonance (SPR) band for the Au nanoparticles. We found a SPR peak for 20 U enzyme, at 549 nm, which gradually blue shifted (lower wavelength) at 536 nm on increasing concentration of the enzyme up to 150 U (**Figure 3B, 3D**). This can be attributed to the formation of different sized nanoparticles.

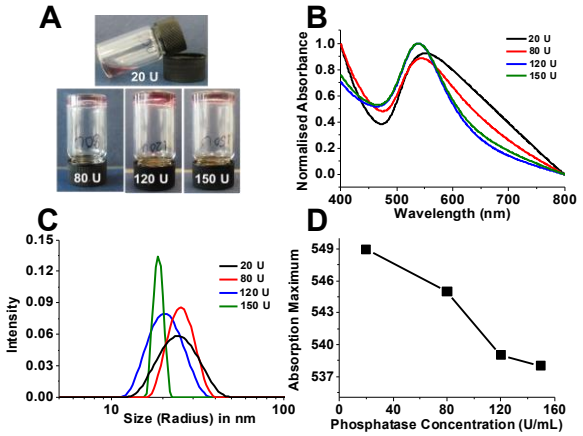

Figure 3. A) Digital images of gold nanoparticle formation with different enzyme concentrations that influence the rate of dephosphorylation. B) UV-visible spectra show different SPR bands of the Au nanoparticles with different enzyme concentrations corresponding to different size of the particles. C) DLS size distribution spectra of the Au nanoparticles at different enzyme concentrations. D) Correlation curve of the absorption maximum of the UV-vis spectra of Au nanoparticles with concentrations of the enzyme used.

We carried out the dynamic light scattering (DLS) studies to determine the size of the particles formed. DLS was performed after filtering the diluted sample in a 150 nm filter to remove the peptide nanofibers (the size of the nanofibers were in micrometer range; **Figure 2E**). DLS (**Figure 3C**) shows that, with increase in phosphatase concentration the size of the Au nanoparticles decreases and the size distribution also narrows for the highest enzyme concentration tested. This observation can be explained by the mechanism of the particle formation that at high enzyme concentration, at early time points, there are more free phenolic hydroxyl groups available for the reduction and nucleation of the particles, which is reflected in the smaller size of the particles. Transmission electron microscope also confirms the size dependence (**Figure S7**). At higher enzyme concentration (150U), we found smaller particles (35-45 nm) (**Figure S7A**). Similarly with decrease in enzyme concentration 120U, 80 and 20U we found 45-70 nm, 55-80 nm and 70-110 nm particle size respectively as demonstrated in **Figure S7**B,C,D respectively.

To assess the role of kinetics, the biocatalytic conversion and the initial rate of self-assembly in the size control, chemical self-assembly of Fmoc-FY (synthesized as compiled in **Figure S1**; synthetic details and characterization (**NMR**) are provided in supporting information (**Figures S1-S5**).) was explored by dissolving the peptide (20 mM) in aqueous solution at a final pH 8. Upon addition of Au (III) chloride solution, initially the reaction mixture became colourless (Au (I)), and then it turned into pink/red/violet (Au (0)), At high Au (III) concentration (20mM; [Fmoc-FY-OH]:[Au(III)] = 1:1), the reduction was found to be incomplete and it lead to the formation of colourless Au (I). By reducing the concentration of Au (III), the reduction reached to the completion to Au (0) to form Au nanoparticles. The reduction was found to be fast and the color changes take place in 2 h (**Figure S8A**). These particles were found to be further stabilized by the self-assembled hydrogel network. They showed a broad surface plasmon resonance band at ~515 nm, characteristics of Au nanoparticles (**Figure S8B**). In order to examine whether the presence of enzyme protein (present at varying concentration and proteins have been used before to template NP formation [31]) plays a role in determining the size of nanoparticles, we added different phosphatase concentrations (20-150U) to Fmoc-FY-OH solution during the self-assembly process (*i.e.* the enzyme is a spectator here, as no dephosphorylation is required). UV-vis was performed on all the samples after 48h. It was found out that all the samples have a broad SPR band around 510-515 nm, suggesting that, it is the biocatalytic self-assembly kinetics and not the protein concentration that controls the size of the gold nanoparticles formed. The sizes of the nanoparticles are found to be in the range of (10-15 nm) using electron microscopy (**Figure S8C**). In another control experiment to confirm whether enzyme phosphatase itself has any role in reduction of gold chloride, we added different concentrations of phosphatase (20U-150U) to gold chloride solution without any peptide. We observed no gold nanoparticle formation as there is no absorption for gold nanoparticles as seen in UV-Vis spectroscopy (**Figure S9**).

In order to establish whether the catalytic controlled exposure of phenol groups alone is responsible for the size control of the particles formed, we used a water-soluble analogue O-phospho-L-tyrosine to investigate the role of gelation on the size and properties of the nanoparticles formed. The molecule can be hydrolyzed by phosphatase thereby exposing a tyrosine moiety but does not form a nanofiber network (**Figure S10**). Phosphatase was used to cleave the phosphate group to reveal the soluble tyrosine residue. A change in color from yellow to blue was observed (**Figure S10B**) and using UV-vis spectroscopy after 48h of adding the Au (III) chloride solutions we observe a broad SPR band (**Figure S10C**). TEM analysis revealed that, although there are some nanoclusters formed (due to reduction by tyrosine moiety), they do not have any definite size and shape (**Figure S10D**).

It could be concluded from these control experiments that while the concentration of phosphatase play a role in controlling the size of the nanoparticles, the presence of hydrogel (as a template) is essential in stabilizing the nanoparticles formed with monodispersity of the gold nanoparticles enhanced in presence of hydrogel network (**Figure S11**). Notably, the nanoparticles formed within a hydrogel template are stable for months, whereas the nanoparticles formed without any hydrogel network are not stable and the particle settle down in the bottom of the glass vial after few days (**Figure S12**).This suggests the significance of the fibrous network for the synthesis and stabilization of the nanoparticles where aggregation is avoided through association of particles with the nanofibers that are formed which act to stabilize the synthesized nanoparticles.

CONCLUSION

In conclusion, a novel approach for the synthesis of gold nanoparticles has been reported where the kinetically controlled biocatalytic assembly of an aromatic dipeptide amphiphile (Fmoc-FY-OH) (both chemical and enzymatic) gave rise to formation of a kinetically tunable template for formation of gold nanoparticles. The biocatalytic process and presence of the hydrogel template have cooperative effects and enable the size of the nanoparticles to be tuned by varying the concentrations of the biocatalyst *i.e.* higher the concentration of the enzyme, smaller the size of the nanoparticle. This work provides a novel methodology for the synthesis of metal nanoparticles and more generally it shows that non-equilibrium, pathway selective assembly brings new opportunities for formation of supramolecular materials with tunable structure and functionality.

Supporting Information

Electronic Support Information is available: Figures S1-S12. This material is available free of charge *via* internet.

AUTHOR INFORMATION

Corresponding Author

Rein.ulijn@asrc.cuny.edu

Present Addresses

WestCHEM, Department of Pure and Applied Chemistry, Technology and Innovation Center, University of Strathclyde, Glasgow, G1 1RD. Advanced science research centre (ASRC) and Hunter College, City university of New York, NY 10031, NY, USA.

Notes

The authors declare no competing financial interest.

ACKNOWLEDGMENT

We thank the BBSRC for funding (BB/K007513/1). The research leading to these results has received funding from the European Research Council under the European Union's Seventh Framework Programme, ERC (Starting Grant EMERgE) grant agreement no. 258775. This material is based upon work supported by, or in part by, the U.S. Army Research Laboratory and the U.S. Army Research Office under contract/grant W911NF-16-1-0113.

REFERENCES

(1) Whitesides, G. M.; Grzybowski, B. *Science***2002**, *295*, 2418.
(2) Lehn, J.-M. *Science***2002**, *295*, 2400.
(3) Du, X.; Zhou,J.; Shi,J.; Xu,B. *Chem. Rev*.**2015**, *115*, 13165.
(4) Busheron,E.; Ruff,Y.; Moulin,E.; Giuseppone,N. *Nanoscale* **2013**, *5*, 7098.
(5) Mattia, E.; Otto, S. *Nat.Nanotechnol*.**2015**, 10, 111-119.
(6) Tantakitti, F.; Boekhoven, J.; Wang, X.; Kazantsev, R. V.; Yu, T.; Li, J.; Zhuang, E.; Zandi, R.; Ortony, J. H.; Newcomb, C. J.; Palmer, L. C.; Shekhawat, G. S.; de la Cruz, M.; Schatz, G. C.; Stupp, S. I. *Nat. Mater*.**2016**, *15*, 469-476.
(7) Foster, J. S.; Zurek, J. M.; Almeida, N. M. S.; Hendriksen, W. E.; le Sage, V. A. A.; Laxminarayana, V.; Thompson, A. L.; Banerjee, R.; Eelkema, R.; Mulvana, H.; Paterson, M. J.; van Esch, Jan H.; Lloyd, G. O. *J. Am. Chem. Soc*.**2015**, *137(45)*, 14236.
(8) Raeburn, J.; Cardoso, A. Z.; Adams, D. J. *Chem. Soc. Rev*.**2013**, *42*, 5143.
(9) Sahoo, J. K.; Nalluri, S. K. M.; Javid, N.; Webb, H.; Ulijn, R. V. *Chem. Commun.***2014**, *50*, 5462.
(10) Y. Tidhar, H. Weissman, S. G. Wolf, A. Gulino, B. Rybtchinski, *Chem. Eur. J.***2011**, *17*, 6068.
(11) Hirst, A. R.; Roy, S.; Arora, M.; Das, A. K.; Hodson, N.; Murray, P.; Marshall, S.; Javid, N.; Sefcik, J.; Boekhoven, J., van Esch, J. H.; Santabarbara, S.; Hunt, N. T.; Ulijn, R. V.*Nat. Chem.***2010**, *2*, 1089.
(12) Boekhoven, J.; Poolman, J. M.; Maity, C.; Li, F.; van der Mee, L.; Minkenberg, C. B.; Mendes, E.; van Esch, Jan H.; Eelkema, R. *Nat. Chem*. **2013**, *5*, 433.
(13) Yang, Z.; Gu, H.; Fu, D.; Gao, P.; Lam, J. K.; Xu, B. *Adv. Mater*.**2004**, *16*, 1440.
(14) Sahoo, J. K.; Pappas, C. G.; Sasselli, I. R.; Abul-Haija, Y. M.; Ulijn, R. V.; *Angew. Chem. Int. Ed.*, **2017**, *56*, 6828.
(15) Zhao, H.; Sen, S.; Udayabhaskararao, T.; Sawczyk, M.; Kučanda, K.; Manna, D.; Kundu, P. K.; Lee, J.-W.; Král, P.; Klajn, R. *Nat.Nanotechnol.***2016**, *11*, 82.
(16) Anker, J. N.; Hall, W. P.; Lyandres, O.; Shah, N. C.; Zhao, J.; van Duyne, R. P. *Nat. Mater.***2008**, *7*, 442.
(17) Rosi, N. L.; Mirkin, C. A. *Chem. Rev*. **2005**, *105*, 1547.
(18) Naik, R. R.; stringer, S. J.; Agrawal, G.; Jones, S. E.; Stone, M. O.*Nat. Mater*. **2002**, *1*, 169.
(19) Slocik, J. M.; Stone, M. O.; Naik, R. R.*Small***2005**, *1*, 1048.
(20) Jackson, E.; Ferrari, M.; Cuestas-Ayllon, C.; Fernandez-Pacheco, R.; Perez-Carvajal, J.; de la Fuente, J. M.; Grazu, V.; Betancor, L.*Langmuir***2015**, *31*, 3687.
(21) Li, Z.; Chung, S-W.; Nam, J-M.; Ginger, D. S.; Mirkin, C. A. *Angew. Chem*.**2003**, *115*, 2408.
(22) Ray, S.; Das, A. K.; Banerjee, A. *Chem. Commun*.**2006**, 2816.
(23) Vemula, P. K.; John, G.*Chem. Commun*.**2006**, 2218.
(24) Mitra, R. N.; Das, P. K.*J. Phys. Chem. C***2008**, *112*, 8159.
(25) Adhikari, B.; Banerjee, A.*Chem. Eur. J*. **2010**,*16*, 13698.
(26) Zayats, M.; Baron, R.; popov, I.; Willner, I. *Nano. Lett*.**2005**, *5*, 21.
(27) Fleming, S.; Ulijn, R. V.*Chem. Soc. Rev*.**2014**, *43*, 8150.
(28) Sadownik, J.W.; LeckieJ. and Ulijn, R.V. *Chem. Commun*.,**2011**, 47, 728-730.
(29) Bhargava, S. K.; Booth, J. M.; Agrawal, S.; Coloe, P.; Kar, G., *Langmuir***2005**, *21*, 5949.
(30) Xie, J.; Lee, J. Y.; Wang, D. I. C.; Ting, Y. P., *ACS Nano***2007**, *1*(5), 429.
(31) McMillan, R. A.; Pavola, C. D.; Howard, J.; Chan, Zaluzec, N. J.; Trent, J. D.*Nat. Mater*.**2002**, *1*, 247.